Geosci. Model Dev. Discuss., 6, 1223–1257, 2013
www.geosci-model-dev-discuss.net/6/1223/2013/
doi:10.5194/gmdd-6-1223-2013

Geoscientific Model Development Discussions
Open Access

An online trajectory module (version 1.0) for the non-hydrostatic numerical weather prediction model COSMO

A. K. Miltenberger, S. Pfahl, and H. Wernli

Institute for Atmospheric and Climate Science, ETH Zurich, Switzerland

Received: 29 January 2013 – Accepted: 4 February 2013 – Published: 21 February 2013

Correspondence to: A. K. Miltenberger (annette.miltenberger@env.ethz.ch)

Published by Copernicus Publications on behalf of the European Geosciences Union.

Abstract

A module to calculate online trajectories has been implemented into the non-hydrostatic limited-area weather prediction and climate model COSMO. Whereas offline trajectories are calculated with wind fields from model output, which is typically available every one to six hours, online trajectories use the simulated wind field at every model time step (typically less than a minute) to solve the trajectory equation. As a consequence, online trajectories much better capture the short-term temporal fluctuations of the wind field, which is particularly important for mesoscale flows near topography and convective clouds, and they do not suffer from temporal interpolation errors between model output times. The numerical implementation of online trajectories in the COSMO model is based upon an established offline trajectory tool and takes full account of the horizontal domain decomposition that is used for parallelization of the COSMO model. Although a perfect workload balance cannot be achieved for the trajectory module (due to the fact that trajectory positions are not necessarily equally distributed over the model domain), the additional computational costs are fairly small for high-resolution simulations. Various options have been implemented to initialize online trajectories at different locations and times during the model simulation. As a first application of the new COSMO module an Alpine North Föhn event in summer 1987 has been simulated with horizontal resolutions of 2.2 km, 7 km, and 14 km. It is shown that low-tropospheric trajectories calculated offline with one- to six-hourly wind fields can significantly deviate from trajectories calculated online. Deviations increase with decreasing model grid spacing and are particularly large in regions of deep convection and strong orographic flow distortion. On average, for this particular case study, horizontal and vertical positions between online and offline trajectories differed by 50–190 km and 150–750 m, respectively, after 24 h. This first application illustrates the potential for Lagrangian studies of mesoscale flows in high-resolution convection-resolving simulations using online trajectories.

GMDD
6, 1223–1257, 2013

1 Introduction

The Lagrangian depiction of atmospheric processes has a long tradition in atmospheric sciences: the first dynamic studies date back to the beginning of the 20th century when Shaw et al. (1903) and Shaw and Lempfert (1906) used trajectories to describe the motion of air parcels in cyclones. These first trajectories were so-called surface trajectories, which took into account only the wind fields close to the earth surface. Later trajectories were calculated on isobaric surfaces and, when the importance of vertical motion of air parcels became evident, also on isentropic surfaces (Danielsen, 1961). As trajectories calculated on isentropic surfaces can only represent adiabatic motions, three-dimensional trajectories using all three components of the wind field were introduced (e.g. Reap, 1972). These three-dimensional kinematic trajectories became especially popular since the late 1980s when good quality and well resolved gridded wind fields became available. They are nowadays considered to be the most accurate type of trajectories in the troposphere (Stohl and Seibert, 1998). From the early studies on, the Lagrangian perspective had a large impact on the advance of the understanding of atmospheric processes, as for instance it allowed to identify coherent air streams that occur within extratropical cyclones, most prominently the warm conveyor belt (e.g. Whitaker et al., 1988; Wernli and Davies, 1997). Lagrangian studies were also important to connect ozone-rich episodes in the troposphere to stratospheric intrusions (e.g. Buzzi et al., 1984), or to illustrate the flow blocking at mountain ranges during the passage of fronts (e.g. Buzzi and Tibaldi, 1978; Steinacker, 1984; Kljun et al., 2001). Since trajectory calculations are computationally cheap, the Lagrangian approach is also very valuable to assess the climatological frequency and geographical distribution of atmospheric flow features like warm conveyor belts (e.g. Eckhardt et al., 2004) or stratosphere-troposphere exchange (e.g. Sprenger and Wernli, 2003). But trajectory analysis also made its way to other fields of atmospheric sciences: for instance it was successfully used for analyzing the detailed microphysical evolution of clouds along the flow (e.g. Haag and Kärcher, 2004; Hoyle et al., 2005; Brabec et al., 2012), identifying

GMDD
6, 1223–1257, 2013

evaporative water sources for precipitation (e.g. Bertò et al., 2004; Sodemann et al., 2008), interpreting measurements of stable water isotopes (Pfahl and Wernli, 2008) and in studies on atmospheric chemistry (e.g. Coude-Gaussen et al., 1987; Miller, 1987; Forrer et al., 2000; Methven et al., 2006).

While frequently employed in all fields of meteorology, the accuracy of trajectories derived from measured or modeled wind data is a long standing point of discussion (e.g. Danielsen, 1961; Kahl, 1993; Stohl, 1998; Brioude et al., 2012). The comparison of computed trajectories to the actual path of an air parcel in the atmosphere is difficult, but several attempts have been made for instance with the aid of tracer experiments (e.g. Draxler, 1987; Haagenson et al., 1990; van Dop et al., 1998) and balloon or tetroon flights (e.g. Djuric, 1961; Reisinger and Mueller, 1983; Stohl and Koffi, 1998). In addition to these experiments different trajectory models have been compared (e.g. Stohl et al., 2001), the sensitivity to the input data frequency has been tested (e.g. Rolph and Draxler, 1990; Doty and Perkey, 1993; Stohl et al., 1995) and the errors associated with the numerical scheme have been investigated (Seibert, 1990). In the case of three-dimensional kinematic trajectories, which are usually based on wind data from a reanalysis data set or a numerical weather prediction model, several error sources can be identified (Stohl, 1998):

1. truncation errors: due to neglecting higher order terms in the Taylor expansion of the trajectory equation
2. interpolation errors: due to the interpolation of the wind field data from the model grid and model output times to the actual trajectory position in space and time
3. wind field errors: due to prediction errors in the wind field
4. starting position errors (e.g. relevant for modeling dispersion of a released substance)

The last two error sources depend largely on the quality of the entire forecasting system and the precision of the initial conditions, which are independent of the trajectory

GMDD
6, 1223–1257, 2013

model. The truncation error depends on the numerical scheme used for solving the trajectory equation. All of today's frequently used trajectory models, FLEXPART (Stohl et al., 2005), HYSPLIT (Draxler and Hess, 1998), TRAJKS (Scheele et al., 1996), and LAGRANTO (Wernli and Davies, 1997), employ the Petterssen scheme (Petterssen, 1940), which is a second-order scheme, i.e. the truncation error is proportional to Δt^2. For further discussion of the numerical properties the reader is referred to Seibert (1990). As the Petterssen scheme is second order a short integration time step Δt is favorable, which in turn requires a high temporal resolution of the wind field data. All of the above-mentioned models compute the trajectories based on winds from numerical weather prediction model simulations or reanalysis data sets. Typically, output from global models (analyses and forecasts) is available every 6 h, and from regional models every hour. As integration time steps of this order would induce unacceptably large errors, temporal interpolation between these output times is required for calculating trajectories.

The errors introduced by temporal and spatial interpolation depend strongly on the temporal and spatial resolution of the wind data. While the spatial resolution of numerical weather prediction models has strongly increased over the past years, the output frequency has increased only slowly and therefore often constitutes the limiting factor for a reduction of the interpolation error. Both the truncation and the temporal interpolation error can be reduced to a minimum if the trajectory equation is solved "online", i.e. during the integration of the Eulerian numerical weather prediction model. In this case the wind fields are available at every time step of the Eulerian model, which is some tens of seconds in state-of-the-art regional weather prediction models. Consequently, with this approach a large increase in data resolution is obtained compared to the standard approach of calculating "offline" trajectories. The first implementation of online trajectories we know of has been accomplished by Rössler et al. (1992). They showed in a case study that indeed the increased data input frequency significantly alters the pathways of air parcels particularly over strongly structured topography. More recently the online computation of air parcel trajectories has been utilized in chemistry

GMDD
6, 1223–1257, 2013

models for a Lagrangian advection scheme for trace gases (e.g. Becker and Keuler, 2001; Reithmeier and Sausen, 2002). In addition to the expected improvement of the trajectory position found by Rössler et al. (1992), the online computation of trajectories may better capture the small-scale variability of the vertical wind field as it is represented on the grid of the Eulerian numerical model. As shown in recent studies by Grell et al. (2004) and Brioude et al. (2012) this is especially relevant for regional weather prediction models with a high spatial resolution. A good representation of the small-scale structure of the wind field is important for investigations of orographic flow and deep convection. For studies using the Lagrangian approach to investigate the evolution of clouds or chemical substances it is essential to capture the vertical wind fluctuations: for instance the number of homogeneously nucleating ice crystals is very sensitive to the cooling rates along the trajectory (e.g. Kärcher and Lohmann, 2002; Hoyle et al., 2005; Spichtinger and Krämer, 2012).

In this paper we describe a new implementation of the online computation of trajectories in the regional weather prediction model COSMO (Sect. 2). To illustrate the capabilities of the online trajectory approach, the module is used in a simulation of an Alpine Föhn event in July 1987, which is described in Sect. 3. We provide a comparison of the online trajectories to offline trajectories based on COSMO model output at different output frequencies between one and six hours with a particular emphasis on the representation of the Föhn flow. In addition we investigate the dependence of the detected differences between online and offline trajectories on the horizontal grid spacing of the COSMO model (14 km, 7 km and 2.2 km). Finally in Sect. 4 potentials of and challenges for the online computation of trajectories are discussed.

2 The online trajectory module

For the implementation of the online trajectory module two existing model codes are combined: on the one hand we select the numerical weather prediction model COSMO as the Eulerian model into which the online trajectory calculation should be embedded.

GMDD
6, 1223–1257, 2013

The COSMO model is a limited area, non-hydrostatic model (Steppeler et al., 2003), which is used for high resolution operational weather forecasting by several mainly European weather services (e.g. Deutscher Wetterdienst and MeteoSwiss). On the other hand we base the trajectory calculation procedure (time stepping as well as interpolation) on the trajectory tool LAGRANTO (Wernli and Davies, 1997), which has been employed in numerous studies to compute offline trajectories (e.g. Wernli and Davies, 1997; Kljun et al., 2001; Stohl et al., 2001; Hoyle et al., 2005).

The major technical criteria for the design of the online trajectory module are (i) to make as little changes to the existing COSMO source code as possible, (ii) to write a module which does not rely heavily on existing COSMO source code to make its adaption to other numerical weather prediction models straightforward and (iii) to obtain a reasonable computational performance of the COSMO model with the online trajectory module. In the present version the trajectory module inherits from the COSMO model only the spatial grid decomposition and partly relies on the IO-structure of the COSMO model for the output of trajectory data. With the setup described below only few additional lines have to be added to the existing code. In the namelist used for starting the COSMO model an additional switch is introduced, which allows to shut on or off the trajectory calculation, and an additional namelist block allows the user to specify essential parameters of the module like the starting region, the time step for the output and the traced variables.

The general workflow inside the module and its embedding in the existing model is illustrated by the flow chart in Fig. 1: after initialization of the COSMO model and the trajectory module (Sect. 2.3), the model loops through the time steps of the integration. At the end of each time step the trajectory module is called to calculate the new trajectory positions (Sect. 2.1). Then the necessary inter-processor communication takes place (Sect. 2.2) and finally, if the time step is an output time step, the trace variables are interpolated to the trajectory positions and are together with the trajectory position written to the output files.

GMDD
6, 1223–1257, 2013

2.1 Physical core

The physical core has to solve the trajectory equation $\frac{Dx}{Dt} = \boldsymbol{u}(\boldsymbol{x}, t)$. For the solution of this equation we employ the Petterssen scheme (Petterssen, 1940), which computes the new trajectory position at time $t_1 = t_0 + \Delta t$ from the externally specified velocity $\boldsymbol{u}(\boldsymbol{x}, t)$ by using an iterative forward Euler time step:

$$\boldsymbol{x}_1(t_1) \approx \boldsymbol{x}(t_0) + \Delta t \boldsymbol{u}(\boldsymbol{x}, t_0)$$

$$\boldsymbol{x}_2(t_1) \approx \boldsymbol{x}(t_0) + \frac{1}{2}\Delta t \left(\boldsymbol{u}(\boldsymbol{x}, t_0) + \boldsymbol{u}(\boldsymbol{x}_1, t_1)\right)$$

$$\ldots$$

$$\boldsymbol{x}_n(t_1) \approx \boldsymbol{x}(t_0) + \frac{1}{2}\Delta t \left(\boldsymbol{u}(\boldsymbol{x}, t_0) + \boldsymbol{u}(\boldsymbol{x}_{n-1}, t_1)\right)$$

We choose this scheme because it is used by all of the frequently used trajectory models, because it is accurate to the second order and because several studies have shown that higher order schemes do not perform essentially better (e.g. Seibert, 1990). It should be noted that the Petterssen scheme is a so-called "constant acceleration" solution, i.e. it neglects the change in acceleration of the air parcel during an integration time step. However, we think that this assumption is justified in the online computation even more than in the offline calculation because of the very small integration time step. The number of iterations required for convergence depends on the flow situation and the time step, but we find that a default value of three iterations gives mostly satisfactory results. However, it is possible to alter this number via the namelist.

The Petterssen scheme requires the velocity $\boldsymbol{u}(\boldsymbol{x}, t)$ at the parcel location at each integration time step and therefore an interpolation of the wind data on the Eulerian grid to the parcel position is necessary. We decided to use a three-dimensional linear interpolation as it is, for instance, also used in LAGRANTO. Higher order interpolation is used by some other trajectory models (e.g. FLEXPART, optional in LAGRANTO), but may not always give better results. Moreover the errors introduced by the linear

GMDD
6, 1223–1257, 2013

interpolation are much easier to interpret. In contrast to existing offline models, no temporal interpolation of the wind field is required as it is available at each model time step, which is for online trajectories identical to the trajectory integration time step.

Despite the strong increase of the temporal resolution of trajectories and wind field data, some trajectories are advected below the ground in the online approach due to numerical errors, spatial interpolation errors and the neglected turbulence. To avoid losing trajectories close to the surface we use a jump flag, which artificially places the trajectories 10 m above the surface if they hit the topography (for a more detailed discussion see Sect. 4).

2.2 Parallelization and communication

The COSMO model employs a spatial grid decomposition for the computation on multi-processor machines, which constitutes a major difficulty for introducing the trajectory calculation: in contrast to the Eulerian model, for which the grid points have a fixed spatial position, i.e. remain associated with a certain processor during the entire integration, trajectories have no fixed spatial position and hence may pass from the spatial domain associated to a certain processor to another domain. This problem increases the inter-processor communication significantly, which may deteriorate the model performance on multi-processor machines. In addition the trajectories may not be equally distributed in space at each time instant, which makes it impossible to obtain a workload balance, without strongly modifying the existing COSMO model structure. However, the effects of the workload imbalance may not strongly affect the model performance because usually the number of operations needed on a certain processor to compute the new trajectory positions is much less than the number of operations required at the Eulerian grid points. Most important, in case of a dynamical association of the grid points to processors parts of the Eulerian variable fields have to be exchanged between processors at each time step. This additional communication is computationally expensive and would offset the effect of a perfect workload balance in almost all applications. We therefore decided to keep a fixed spatial domain decomposition.

GMDD
6, 1223–1257, 2013

The trajectory locations are stored in an array, which is apriori known to all processors. A certain processor works only on the entries corresponding to trajectories inside its domain. However, in order to minimize the communication, the trajectory array is only updated at the processor that performs the integration, and in case that a trajectory passes to the domain of another processor the information is transfered to this other processor. As illustrated in Fig. 1 all communications are performed when all processors have finished the forward integration. This allows to obtain a minimum number of communication operations and therefore reduces the communication overhead. Additional communication is required if output has to be written at a certain time step, because then the entire trajectory array on the processor responsible for the IO has to be updated. In some cases with very few trajectories passing between processors a complete update of the trajectory array on all processors after each time step may be faster due to a smaller relative communicational overhead. Therefore this option is also implemented. For all communications the MPI-library is used as in the entire COSMO model.

2.3 Initialization

An essential choice made by the user of the online trajectory module is the specification of the starting points of the trajectories. This is not a trivial task as no backward computation is possible and hence an apriori knowledge of the interesting starting regions and times is required. Starting trajectories at all grid points and time steps is not feasible for high-resolution models due to storage limitations and because it will very strongly increase the runtime of the model. In the present version several options to specify the starting region are available:

- start trajectories once at each gridpoint inside a rectangular box (via namelist)
- start trajectories once at user-specified coordinates (via external file)
- start trajectories at fixed locations at user-specified times (via namelist)

GMDD
6, 1223–1257, 2013

– start trajectories repeatedly at fixed locations at a regular time interval (via namelist)

– start trajectories at different locations at different times (via external file)

3 Results from an Alpine case study

For a first application of the new online trajectory module we simulate the meteorological evolution over Central Europe from 25 to 29 July 1987, which has already been investigated by Rössler et al. (1992), Buzzi and Alberoni (1992) and Paccagnella et al. (1992).

3.1 Meteorological situation

On 25 July 1987 an upper-level trough was located over Central Europe and the Mediterranean, and mostly northerly flow prevailed in this region. In the following two days the trough propagated eastward. On 26 July 1987 the associated surface cold front reached the Alps and was strongly deformed due to the influence of the Alpine orography: along the Rhone valley a strong Mistral was observed, some portions of the cold air spilled over the Alpine ridge and induced North Föhn in Ticino and northern Italy, and finally along the eastern edge of the Alps a low-level jet formed (Buzzi and Alberoni, 1992). As the cold air propagating around the eastern edge of the Alps met the warmer air over the eastern Po Valley, deep convection developed along the convergence line in the afternoon of the 26 July (Buzzi and Alberoni, 1992). In addition a moderate Alpine lee cyclone developed over the Adriatic Sea, which was influenced by the retardation and deformation of the cold front by the Alpine ridge (Buzzi and Alberoni, 1992). For the trajectory analysis we focus on the time period during which the cold front passes the Alps, i.e. the afternoon and evening of 26 July 1987.

GMDD
6, 1223–1257, 2013

3.2 Modeling framework

For the numerical simulations of the case study the COSMO model version 4.17 (Steppeler et al., 2003) is used with three different spatial resolutions: with 40 vertical levels and a horizontal grid spacing of 14 km (195 × 200 grid points, COSMO14) and 7 km (390 × 400 grid points, COSMO7), and with 60 vertical levels and a horizontal grid spacing of 2.2 km (1190 × 1220 grid points, COSMO2.2), respectively. The domain reaches from approximately 30° N to 55° N and from 7° W to 25° E. We employ the standard model setup of the Swiss weather service except for the microphysical parameterization, for which the two-moment scheme by Seifert and Beheng (2006) is used. For the COSMO2.2 simulation only shallow convection is parameterized, while in the other simulations also deep convection is parameterized. The time step is 20 s for COSMO2.2 and 40 s for the two other setups. The boundary and initial conditions for COSMO14 and COSMO7 are derived from the ERA40 reanalysis with a spatial resolution of T159 (Uppala et al., 2005), while COSMO2.2 is driven by the COSMO7 simulation. Therefore the COSMO2.2 simulation is performed over a slightly smaller geographical domain. The COSMO14 and COSMO7 simulations are started at 00:00 UTC 25 July 1987, COSMO2.2 is started 2 h later. All simulations end at 00:00 UTC 29 July 1987. Each simulation is performed twice, once with and once without the online trajectory module. In total 24 615 trajectories are started over the British Isles at each model level from the surface up to 5 km at 02:00 UTC 25 July 1987. According to the distribution of vertical levels in the Gal-Chen hybrid coordinate system this gives about twice as many trajectories starting below 2 km than above.

A comparison of the sea-level pressure, temperature and precipitation evolution simulated by the COSMO model with the analysis by Buzzi and Alberoni (1992) and Paccagnella et al. (1992) reveals a reasonable performance for all simulations (not shown). The developing lee cyclone is slightly shallower than in the observations and the convection over the eastern Po Valley starts about three hours later. Nevertheless, the essential mesoscale phenomena like the Föhn flow, a strong mistral and the

GMDD
6, 1223–1257, 2013

strong low level jet around the eastern edge of the Alpine ridge are well captured in the COSMO simulations.

For the evaluation of the trajectory module we also compute offline trajectories with LAGRANTO for each model simulation. The offline trajectories are started at the same points and time as the online trajectories. For the integration of the offline trajectories the wind fields from the COSMO simulations are used at output intervals of one, three and six hours and the integration time step is set to one twelfth of this time interval. A jump flag is used for the offline trajectory calculation, similar to the online trajectories.

3.3 Computational performance of the online trajectory module

To assess the computational performance of the COSMO model with the online trajectory module we use the model simulations performed for the Alpine case study described in the previous section. The number of processors varies with the spatial resolution of the simulation to obtain reasonable runtimes: 16 for the 14 km and 7 km simulations and 128 for the 2.2 km simulation, respectively. In addition to the position, 10 additional variables were traced along the online trajectories and all variables are written to the output files every model time step. 22 three-dimensional and 14 two-dimensional Eulerian variables are written to output files every model hour. For more details on the model simulations consider Sect. 3.2.

The results from this performance test are summarized in Table 1. For this specific setup the runtime increase due to the trajectory module is below 30 % for the 14 km simulation, and the impact of the trajectory calculation on the runtime decreases to a few percent for the higher-resolution simulations. This is because the number of trajectories remains constant while the number of grid points is much larger. Of course the expected runtime increase strongly depends on the number of trajectories, the number of traced variables and the number of processors. In general the observed run time increase is satisfactorily small in this test case.

GMDD
6, 1223–1257, 2013

3.4 Comparison of online and offline trajectories

The most prominent mesoscale flow features identified by Buzzi and Alberoni (1992), the flow splitting at the Alps with a strong low-level wind on either side of the mountain range and the North Föhn flow with a particularly strong outflow from the Simplon-Gotthard region, are well captured by the online and offline trajectory calculations (Fig. 2, Föhn trajectories are those passing close by the black star in both panels). Another interesting feature revealed by the trajectory analysis is the strongly ascending branch of air over eastern Europe, which is associated with ascent ahead of the upper-level trough. Its passage over Central Europe is accompanied by trajectories suddenly changing direction from southeast to northeast and rising as for instance also observed over the eastern Alps (trajectories rising above 5 km in Fig. 2). A first qualitative impression of the differences between online and offline trajectories can be obtained from Fig. 2: while on first order the flow patterns of the online (bottom panel) and the offline trajectories based on three-hourly output (top panel) agree quite well, significant differences are observable if sub-synoptic scale flow patterns are considered. For instance the flow around Corsica shows a much more detailed flow structure in the online trajectories, the ratio of trajectories passing over and around the Massif Central, the Pyrenees and the Alps varies quite strongly and over the Po Valley the westward curvature of the online trajectories, which crossed the Alps, is much stronger than that of the equivalent offline trajectories.

To obtain a more thorough assessment of the path of air parcels calculated from wind fields with different temporal resolutions, trajectories starting at the same location are compared by calculating the average horizontal and vertical transport deviation (AHTD and AVTD). These distance measures are frequently used in the literature to quantify the differences of trajectories in different data sets (e.g. Rolph and Draxler, 1990; Stohl, 1998). The AHTD describes the average over n trajectories of the horizontal distance between each trajectory calculated with two data sets as a function of time after

GMDD
6, 1223–1257, 2013

initialization:

$$\mathrm{AHTD}(t) = \frac{1}{N}\sum_{n=1}^{N}\left((X_n(t) - x_n(t))^2 + (Y_n(t) - y_n(t))^2\right)^{0.5}$$

where (x_n, y_n) is the position of the nth reference trajectory and (X_n, Y_n) the position of the nth test trajectory. The AVTD is calculated with a similar equation for the trajectory heights z_n and Z_n instead of the horizontal position. Note that, AHTD and AVTD only indicates the mean deviation of all pairs at a certain time. The sensitivity of trajectories with the same starting point to the temporal resolution of the wind field data can vary substantially with the flow features they encounter during their path: as illustrated in Fig. 3 online and offline trajectories sometimes take almost the same path, while at other occasions they diverge strongly and spread over entire Europe. It appears that the closer to the starting point a sensitive flow situation is encountered, the larger is the final deviation. For instance the strongly diverging trajectory bundle shown in Fig. 3 (solid lines) enters a convective region off the coast of northern France. In this case the representation of small-scale vertical velocity structures strongly influences the final three-dimensional path of the parcel. The other set of trajectories shown in Fig. 3 (dashed-dotted lines) does not encounter such a sensitive situation and remains fairly coherent.

AHTD and AVTD were computed with the online trajectories as the reference data set and offline trajectories as the test data set for all spatial and temporal resolutions used in this case study (Fig. 4). In addition online trajectories for simulations with different spatial resolutions are compared to assess the influence of a changing horizontal model resolution (Fig. 4, red lines). In all cases the AHTD increases more or less steadily with increasing simulation time, which can be explained by the increasing divergence of the trajectories once they enter specific flow regions. The AVTD increase is much less steady, which is probably due to the more localized structure of strong vertical winds; the strongest increases in AVTD occur during times, when many trajectories pass over steep topography.

GMDD
6, 1223–1257, 2013

Comparing the AHTD and AVTD evolution for the same spatial resolution, but different data input frequencies for the offline trajectories (same line style in cyan, green and blue in Fig. 4) indicates a weaker deviation between offline and online trajectories with increasing temporal resolution of the wind fields used for the offline trajectories: for instance, if COSMO7 results are considered, the AHTD after 24 h (48 h) is 127 km (393 km) for six-hourly offline trajectories, 97 km (329 km) for three-hourly offline trajectories and 61 km (256 km) for one-hourly offline trajectories. For the spatial resolution of the wind fields the opposite behavior is observed: AHTD and AVTD are smallest for the COSMO14 simulation and largest for the COSMO2.2 simulation: for example, if one-hourly offline trajectories are used as reference, the AHTD after 24 h (48 h) is 50 km (214 km) for COSMO14 based trajectories, 61 km (256 km) for COSMO7 and 133 km (444 km) for COSMO2.2. This is most likely related to the differences in atmospheric dynamics depending on the spatial resolution: while for the coarsest resolution the flow should be largely hydrostatic, the flow in the COSMO7 simulation has a non-hydrostatic component, and in the COSMO2.2 simulation even deep convective motion is explicitly resolved on the Eulerian grid. The offline trajectory method performs worse in finding an accurate numerical solution to the trajectory equation if the flow is less homogeneous in space and time. A comparison of online trajectories based on COSMO simulations with different spatial resolutions confirms that the sensitivity of trajectories to the temporal resolution gets larger with increasing spatial resolution (red lines in Fig. 4): AHTD and AVTD are smaller if the COSMO7 online trajectories are used as reference instead of the COSMO2.2 online trajectories. Furthermore the explicit representation of deep convective motion in COSMO2.2 has a stronger impact on trajectories than the flow differences between COSMO14 and COSMO7. We conclude this from the fact that the AHTD and AVTD evolution for COSMO14 and COSMO7 online trajectories as test and COSMO2.2 online trajectories as reference are very similar.

The total error after four days forward integration is between 600 km and 900 km in the horizontal (extrapolating the COSMO2.2 results) and between 700 m and 1000 m in the vertical. The AHTD and AVTD values found in the comparison between online

GMDD
6, 1223–1257, 2013

and offline trajectories are somewhat larger than those found in other studies trying to estimate the accuracy of trajectories by comparison of different offline trajectory data sets: Rolph and Draxler (1990) found an AHTD of about 400–500 km after 96 h integration for offline trajectories based on six-hourly input data and Kröner (2011) found an AHTD between 300–600 km after 96 h integration for offline trajectories based on three-hourly and six-hourly input data. The discrepancy may have three reasons: first, both cited studies used wind fields with much coarser spatial resolutions (50 km to 360 km) than applied here and it is obvious from our results that the errors are smaller if wind fields with coarser spatial resolution are considered. Secondly, Rolph and Draxler (1990) and Kröner (2011) averaged trajectories from different synoptic conditions and over different regions (North America respectively the entire Northern Hemisphere) for their comparison. This is anticipated to reduce the average error, as many meteorological conditions are less complex and variable than the crossing of a cold front over the Alps. Finally, they used offline trajectories based on one-hourly wind data as reference data set for their evaluation, which are potentially affected by significant errors. In our case study we found that using offline trajectories based on one-hourly wind data as reference decreases the final AHTD by about 50 km to 100 km and the final AVTD by about 50 m to 100 m (not shown). Therefore it would be desirable to find a more objective way for estimating the errors of trajectories than using one or the other trajectory data set as reference.

3.5 Föhn flow over the Alps

The analysis of the online and offline trajectories indicates that the differences are particularly large for mesoscale flow features. As in addition trajectories have been used quite frequently to study orographic flows in the Alps (e.g. Kljun et al., 2001; Würsch, 2009; Roch, 2011), we decided to perform a more detailed analysis of the representation of the North Föhn flow in the different trajectory data sets. In each data set all trajectories that reached a minimum elevation below 1500 m over the Po Valley after crossing the Alps were selected as Föhn trajectories.

GMDD
6, 1223–1257, 2013

One of the most interesting features of the trajectories is the change in elevation across the Alpine ridge, which has significant implications for the long-standing discussion about föhn mechanisms (e.g. Steinacker, 2006; Drobinski et al., 2007). The elevation change of trajectories across the Alpine ridge is computed by subtracting the minimum elevation of the Föhn trajectories over the Po Valley from their minimum elevation over the Swiss Plateau. For most Föhn trajectories in all of our trajectory data sets this elevation change (Fig. 5) is positive, which means that the majority of air parcels contributing to the Föhn event descended during the passage of the Alpine ridge. However, the distribution of the elevation change varies on the one hand with the horizontal resolution of the model, but on the other hand also with the data input frequency used for the trajectory calculation (Fig. 5, left panels): for the online trajectories based on the 14 km simulation the distribution is strongly peaked with a maximum around 1500 m, but for the simulations with higher horizontal resolution the distribution becomes flatter and the maximum shifts to about 800–1000 m. If different offline and online trajectory data sets are compared, the shape of the distribution changes strongly: offline trajectories based on six- and three-hourly output data show a rather flat distribution of the elevation change, but for offline trajectories based on one-hourly output data and online trajectories there is a clear peak around 800–1000 m elevation change.

The comparison of the distributions of elevation south of the Alps (Fig. 5, right panels) for different data input frequencies shows a similar pattern as for the elevation change across the Alps. However, here the distribution for offline trajectories based on one-hourly output data and for online trajectories differs significantly for elevations below 500 m: while the online trajectories show a structure reminiscent of a low-level jet with a core just below 500 m, no such features is visible in the other data sets. This "low-level jet" is only captured in the COSMO2.2 online trajectories, at lower temporal resolution the distribution is flatter or the maximum is shifted to higher elevations. The changes in the distribution for online-trajectories from COSMO simulations with different spatial resolutions reflect to a large degree the representation of the low-level jet in

GMDD
6, 1223–1257, 2013

the Eulerian model. It becomes clear that for high-resolution simulations online trajectories are very beneficial for capturing and illustrating the physical processes related to Föhn flow.

4 Potential and challenges

A new module for the non-hydrostatic numerical weather prediction model COSMO has been developed, which calculates air mass trajectories using the gridded model wind field at every time step during the integration of the Eulerian model. With this method no temporal interpolation of the wind field data is required and the trajectory equation is integrated with a very small time step corresponding to the Eulerian model time step. Such a small time step as well as the elimination of the temporal interpolation should make the numerical solution of the trajectory equation more accurate. The new module was tested by simulating an Alpine North Föhn event in July 1987, which exhibited a rich mesoscale phenomenology along the Alpine ridge. Although it is not possible in this study to objectively verify trajectories with measurements, we can conclude that the pattern of the online trajectories is physically meaningful, compares well with offline trajectories on the synoptic scale and resolves many important flow phenomena on the mesoscale. The latter are in general not well represented by offline trajectories, particularly if they are based on low-frequency output data. Capturing smaller scale fluctuations in the wind field does not only add additional details to the trajectories, but also alters their path significantly over the entire simulated period: for our Alpine Föhn case study, after 96 h forward integration an offline trajectory is on average displaced by about 600–900 km in the horizontal (AHTD) and by about 700–1000 m in the vertical (AVTD) compared to the online trajectory with the same starting point.

Besides the clear advantages of the online approach, there are also several challenges that should be kept in mind: first of all the COSMO model cannot be used in backward mode, which means that only forward trajectories can be calculated online. This may slightly complicate studies seeking the explanation of a certain point obser-

GMDD
6, 1223–1257, 2013

vation with the help of the history of the sampled air parcel, as for instance frequently done in air pollution (e.g. Forrer et al., 2000) or cloud studies (e.g. Haag and Kärcher, 2004). A related difficulty is the choice of the starting points in general. Some apriori knowledge about interesting meteorological phenomena and their spatio-temporal occurrence is needed to define the starting points before starting the model simulation. This problem may be negligible for problems dealing for instance with the dispersion of a pollutant from a fixed point source, but is not always trivial for other studies. We think, however, that with a sufficient knowledge of the meteorological situation and a rather dense net of starting positions inside the region of interest, it should be possible to retrieve a good selection of online trajectories from just one model simulation.

An unexpected challenge, tied to the numerical implementation, relates to the problem of trajectories intersecting the terrain: while we expected that the number of terrain intersecting trajectories decreases with the time step used for the solution of the trajectory equation, the opposite effect is observed for the online trajectories. About 5 % more trajectories hit the ground than in the offline trajectory data set based on one-hourly model output (COSMO7). A closer investigation shows that two factors explain this behavior, which can be illustrated by a simple model assuming a "zic-zac" topography and a terrain following wind field (Fig. 6): first, spatial interpolation is still required for online trajectories, which tends to smooth the wind field, so that trajectories are not able to climb to rather isolated peaks in topography. Due to this effect (combined with the truncation error) the "online" and the "offline" trajectory in the example do not follow the terrain at a constant distance, as an analytically calculated trajectory would. Second, because the integration time step is much shorter for online than for offline trajectories, it is more frequently verified whether or not the trajectory is below the surface. This increases the frequency of detecting trajectories below the topography. In the example calculation the offline trajectory would not be classified as terrain intersecting, because the points up- and downwind of the first peak are above topography. In contrast the online trajectory would be classified as terrain intersecting. However, it is obvious that this difference is only due to the frequency at which the position relative

GMDD
6, 1223–1257, 2013

to the topography is checked. As it is rather unsatisfactory to "lose" trajectories during the computation, for the moment being we adopted the approach of other offline trajectory tools to artificially push every parcel hitting the topography to a point 10 m above the surface. This is slightly unphysical, but may be viewed as some representation of turbulence close to the ground, which is neglected otherwise. For the future, we hope to find a more physically justified numerical solution to this problem by either modifying the integration procedure close to the surface or by introducing diffusion and turbulence to the trajectory integration in the boundary layer, e.g. by employing the Langevin equations as in FLEXPART (Stohl et al., 2005).

Despite the challenges associated with the online computation of trajectories, this novel possibility for performing Lagrangian studies is supposed to be useful for high resolution simulations and even mandatory for studying atmospheric phenomena with short temporal and spatial scales, as for instance orographic flows or deep convection. There the advent of so-called convection-resolving weather and climate predictions and the capability of calculating online trajectories can lead to novel insight into the evolution of convective weather systems. For instance, as illustrated in Fig. 7 online trajectories can capture the rapid ascent in cumulonimbus clouds from the boundary layer to the upper troposphere and even provide enough data points during the ascent to study the in-cloud processes. Also the recent work of Stern and Zhang (2013) on the warming of hurricane eyes using offline trajectories based on one minute wind data illustrates the necessity and usefulness of high resolution trajectories in this context. Whether such trajectories are realistic of course depends to a large degree on the quality of the underlying Eulerian model, but such trajectories may also help to validate the Eulerian model in a more process-oriented way. In the future clearly some studies addressing the verification aspect more closely, probably also employing observational data, will be very helpful in assessing the accuracy of the online trajectories.

Acknowledgements. We thank Hanna Joos and Michael Sprenger for their enthusiasm for this work and for interesting and stimulating discussions on many aspects presented in this article, and Axel Seifert for providing the COSMO code including the two-moment microphysics

GMDD
6, 1223–1257, 2013

scheme. ETH is acknowledged for providing the computational resources and for funding the work by ETH Research Grant ETH-38-11-1.

References

Becker, A. and Keuler, K.: Continous four-dimensional source attribution for the Berlin area during two days in July 1994. Part I: The new Euler-Lagrange model system LaMM5, Atmos. Environ., 35, 5497–5508, 2001. 1228

Bertò, A., Buzzi, A., and Zardi, D.: Back-tracking water vapour contribution to a precipitation event over Trentino: a case study, Meteorol. Z., 13, 189–200, 2004. 1226

Brabec, M., Wienhold, F. G., Luo, B. P., Vömel, H., Immler, F., Steiner, P., Hausammann, E., Weers, U., and Peter, T.: Particle backscatter and relative humidity measured across cirrus clouds and comparison with microphysical cirrus modelling, Atmos. Chem. Phys., 12, 9135–9148, doi:10.5194/acp-12-9135-2012, 2012. 1225

Brioude, J., Angevine, W. M., McKeen, S. A., and Hsie, E.-Y.: Numerical uncertainty at mesoscale in a Lagrangian model in complex terrain, Geosci. Model Dev., 5, 1127–1136, doi:10.5194/gmd-5-1127-2012, 2012. 1226, 1228

Buzzi, A. and Alberoni, P. P.: Analysis and numerical modelling of a frontal passage associated with thunderstorm development over the Po Valley and the Adriatic Sea, Meteorol. Atmos. Phys., 48, 205–224, 1992. 1233, 1234, 1236

Buzzi, A. and Tibaldi, S.: Cyclogenesis in the lee of the Alps: a case study, Q. J. Roy. Meteor. Soc., 104, 271–287, 1978. 1225

Buzzi, A., Giovanelli, G., Nanni, T., and Tagliazucca, M.: Study of high ozone concentrations in the troposphere associated with lee cyclogenesis during ALPEX, Beitr. Phys. Atmosph., 57, 380–392, 1984. 1225

Coude-Gaussen, G., Rognon, P., Bergametti, G., Gomes, L., Strauss, B., Gros, J. M., and Coustumer, M. N. L.: Saharan dust on Fuerteventura Island (Canaries): chemical and mineralogical characteristics, air mass trajectories, and probable sources, J. Geophys. Res., 92, 9753–9771, 1987. 1226

Danielsen, E. F.: Trajectories: isobaric, isentropic and actual, J. Meteorol., 18, 479–486, 1961. 1225, 1226

GMDD

6, 1223–1257, 2013

Djuric, D.: On the accuracy of air trajectory computations, J. Meteorol., 18, 597–605, 1961. 1226
Doty, K. G. and Perkey, D. J.: Sensitivity of trajectory calculations to the temporal frequency of wind data, Mon. Weather Rev., 121, 387–401, 1993. 1226
Draxler, R. R.: Sensitivity of a trajectory model to the spatial and temporal resolution of the meteorological data during CAPTEX, J. Clim. Appl. Meteorol., 26, 1577–1588, 1987. 1226
Draxler, R. R. and Hess, G. D.: An overview of the HYSPLIT_4 modelling system for trajectories, dispersion, deposition, Aust. Meteorol. Mag., 47, 295–308, 1998. 1227
Drobinski, P., Steinacker, R., Richner, H., Baumann-Stanzer, K., Beffrey, G., Benech, N., Berger, H., Chimani, B., Dabas, A., Dorninger, M., Dürr, B., Flamant, C., Frioude, M., Furger, M., Gröhn, I., Gubser, S., Gutermann, T., Häberli, C., Häller-Scharnhost, E., Jaubert, G., Lothon, M., Mitev, V., Pechinger, U., Ratheiser, M., Ruffieux, D., Seiz, G., Spatzierer, M., Tschannett, S., Vogt, S., Werner, R., and Zängl, G.: Föhn in the Rhine Valley during MAP: a review of its multiscale dynamics in complex valley geometry, Q. J. Roy. Meteor. Soc., 133, 897–916, 2007. 1240
Eckhardt, S., Stohl, A., Wernli, H., James, P., Forster, C., and Spichtinger, N.: A 15-year climatology of warm conveyor belts, J. Climate, 17, 218–237, 2004. 1225
Forrer, J., Rüttimann, R., Schneiter, D., Fischer, A., Buchmann, B., and Hofer, P.: Variability of trace gases at the high-Alpine site Jungfraujoch caused by meteorological transport processes, J. Geophys. Res., 105, 12241–12251, 2000. 1226, 1242
Grell, G. A., Knoche, R., Peckham, S. E., and McKeen, S. A.: Online versus offline air quality modeling on cloud-resolving scales, Geophys. Res. Lett., 31, L16117, doi:10.1029/2004GL020175, 2004. 1228
Haag, W. and Kärcher, B.: The impact of aerosols and gravity waves on cirrus clouds at midlatitudes, J. Geophys. Res., 109, D12202, doi:10.1029/2004JD004579, 2004. 1225, 1242
Haagenson, P. L., Gao, K., and Kuo, Y.-H.: Evaluation of meteorological analyses, simulations, and long-range transport calculations using ANATEX surface tracer data, J. Appl. Meteorol., 29, 1268–1283, 1990. 1226
Hoyle, C. R., Luo, B. P., and Peter, T.: The origin of high ice crystal number densities in cirrus clouds, J. Atmos. Sci., 66, 508–518, 2005. 1225, 1228, 1229
Kahl, J. D.: A cautionary note on the use of air trajectories in interpreting atmospheric chemistry measurements, Atmos. Environ. A-Gen., 27, 3037–3038, 1993. 1226

GMDD
6, 1223–1257, 2013

Kärcher, B. and Lohmann, U.: A parameterization of cirrus clouds formation: homogeneous freezing of supercooled aerosols, J. Geophys. Res., 107, 4010, doi:10.1029/2001JD000470, 2002. 1228

Kljun, N., Sprenger, M., and Schär, C.: Frontal modification and lee cyclogenesis in the Alps: a case study using the ALPEX reanalysis data set, Meteorol. Atmos. Phys., 78, 89–105, 2001. 1225, 1229, 1239

Kröner, N.: Accuracy of trajectory calculation: dependence on the temporal resolution of the input files, Master thesis, ETH Zurich, 2011. 1239

Methven, J., Arnold, S. R., Stohl, A., Evans, M. J., Avery, M., Law, K., Lewis, A. C., Monks, P. S., Parrish, D. D., Reeves, C. E., Schlager, H., Atlas, E., Blake, D. R., Coe, H., Crosier, J., Flocke, F. M., Holloway, J. S., Hopkins, J. R., McQuaid, J., Purvis, R., Rappenglück, B., Singh, H. B., Watson, N. M., Whalley, L. K., and Williams, P. I.: Estabilishing Lagrangian connections between observations within air masses crossing the Atlantic during the International Consortium for Atmospheric Research on Transport and Transformation experiment, J. Geophys. Res., 111, D23S62, doi:10.1029/2006JD007540, 2006. 1226

Miller, J. M.: The use of back air trajectories in interpreting atmospheric chemistry data: a review and bibliography, NOAA technical memorandum ERL-ARL-155, Air Resources Laboratory, Silver Spring, MD, 1987. 1226

Paccagnella, T., Tibaldi, S., Buizza, R., and Scoccianti, S.: High-resolution numerical modelling of convective precipitation over northern Italy, Meteorol. Atmos. Phys., 50, 143–163, 1992. 1233, 1234

Petterssen, S.: Weather Analysis and Forecasting, McGraw-Hill, New York, 1940. 1227, 1230

Pfahl, S. and Wernli, H.: Air parcel trajectory analysis of stable isotopes in water vapor in the eastern Mediterranean, J. Geophys. Res., 113, D20104, doi:10.1029/2008JD009839, 2008. 1226

Reap, R. M.: An operational three-dimensional trajectory model, J. Appl. Meteorol., 11, 1193–1202, 1972. 1225

Reisinger, L. M. and Mueller, S. F.: Comparison of tetroon and computed trajectories, J. Clim. Appl. Meteorol., 22, 664–672, 1983. 1226

Reithmeier, C. and Sausen, R.: ATTILA: atmospheric tracer transport in a Lagrangian model, Tellus B, 54, 278–299, 2002. 1228

Roch, A.: Orographic blocking in the Alps: a climatologic Lagrangian study, Master thesis, ETH Zurich, 2011. 1239

GMDD
6, 1223–1257, 2013

Rolph, G. D. and Draxler, R. R.: Sensitivity of three-dimensional trajectories to the spatial and temporal densities of the wind field, J. Appl. Meteorol., 29, 1043–1054, 1990. 1226, 1236, 1239

Rössler, C. E., Paccagnella, T., and Tibaldi, S.: A three-dimensional atmospheric trajectory model: application to a case study of Alpine lee cyclogenesis, Meteorol. Atmos. Phys., 50, 211–229, 1992. 1227, 1228, 1233

Scheele, M. P., Siegmund, P. C., and Velthoven, P. F. J.: Sensitivity of trajectories to data resolution and its dependence on the starting point: in or outside a tropopause fold, Meteorol. Appl., 3, 267–273, 1996. 1227

Seibert, P.: Convergence and accuracy of numerical methods for trajectory calculations, J. Appl. Meteorol., 32, 558–566, 1990. 1226, 1227, 1230

Seifert, A. and Beheng, K. D.: A two-moment cloud microphysics parameterization for mixed-phase clouds. Part 1: Model description, Meteorol. Atmos. Phys., 92, 45–66, 2006. 1234

Shaw, N. and Lempfert, R. G. K.: The life history of surface air currents, M. O. Memoir, 174, reprinted in Selected Meteorological Papers of Sir Napier Shaw (London, MacDonald and Co., 1955, 15–131), 1906. 1225

Shaw, W. N., Lempfert, R. G. K., and Brodie, F. J.: The meteorological aspects of the storm of February 26–27, 1903, Q. J. Roy. Meteor. Soc., 29, 233–264, 1903. 1225

Sodemann, H., Schwierz, C., and Wernli, H.: Interannual variability of Greenland winter precipitation sources: Lagrangian moisture diagnostic and North Atlantic Oscillation influence, J. Geophys. Res., 113, D03107, doi:10.1029/2007JD008503, 2008. 1226

Spichtinger, P. and Krämer, M.: Tropical tropopause ice clouds: a dynamic approach to the mystery of low crystal numbers, Atmos. Chem. Phys. Discuss., 12, 28109–28153, doi:10.5194/acpd-12-28109-2012, 2012. 1228

Sprenger, M. and Wernli, H.: A northern hemispheric climatology of cross-tropopause exchange for the EAR15 time period (1979–1993), J. Geophys. Res., 108, 8521, doi:10.1029/2002JD002636, 2003. 1225

Steinacker, R.: Airmass and frontal movement around the Alps, Riv. Meteorol. Aeronau., 43, 85–93, 1984. 1225

Steinacker, R.: Alpiner Föhn – eine neue Strophe zu einem alten Lied, Promet, 32, 3–10, 2006. 1240

GMDD

6, 1223–1257, 2013

Steppeler, J., Doms, G., Schättler, U., Bitzer, H. W., Gassmann, A., Damrath, U., and Gregoric, G.: Meso-gamma scale forecasts using the nonhydrostatic model LM, Meteorol. Atmos. Phys., 82, 75–96, 2003. 1229, 1234

Stern, D. P. and Zhang, F.: How does the eye warm? Part II: Sensitivity to vertical wind shear, and a trajectory analysis, J. Atmos. Sci., in press, 2013. 1243

Stohl, A.: Computation, accuracy and applications of trajectories – a review and bibliography, Atmos. Environ., 32, 947–966, 1998. 1226, 1236

Stohl, A. and Koffi, N. E.: Evaluation of trajectories calculated from ECMWF data against constant volume balloon flights during ETEX, Atmos. Environ., 32, 4151–4156, 1998. 1226

Stohl, A. and Seibert, P.: Accuracy of trajectories as determined from the conservation of meteorological tracers, Q. J. Roy. Meteor. Soc., 124, 1465–1484, 1998. 1225

Stohl, A., Wotawa, G., Seibert, P., and Kromp-Kolb, H.: Interpolation errors in wind fields as a function of spatial and temporal resolution and their impact on different types of kinematic trajectories, J. Appl. Meteorol., 34, 2149–2165, 1995. 1226

Stohl, A., Haimberger, L., Scheele, M. P., and Wernli, H.: An intercomparison of results from three trajectory models, Meteorol. Appl., 8, 127–135, 2001. 1226, 1229

Stohl, A., Forster, C., Frank, A., Seibert, P., and Wotawa, G.: Technical note: The Lagrangian particle dispersion model FLEXPART version 6.2, Atmos. Chem. Phys., 5, 2461–2474, doi:10.5194/acp-5-2461-2005, 2005. 1227, 1243

Uppala, S. M., Kållberg, P. W., Simmons, A. J., Andrae, U., Bechtold, V. D. C., Fiorino, M., Gibson, J. K., Haseler, J., Hernandez, A., Kelly, G. A., Li, X., Onogi, K., Saarinen, S., Sokka, N., Allan, R. P., Andersson, E., Arpe, K., Balmaseda, M. A., Beljaars, A. C. M., Berg, L. V. D., Bidlot, J., Bormann, N., Caires, S., Chevallier, F., Dethof, A., Dragosavac, M., Fisher, M., Fuentes, M., Hagemann, S., Hólm, E., Hoskins, B. J., Isaksen, L., Janssen, P. A. E. M., Jenne, R., Mcnally, A. P., Mahfouf, J.-F., Morcrette, J.-J., Rayner, N. A., Saunders, R. W., Simon, P., Sterl, A., Trenberth, K. E., Untch, A., Vasiljevic, D., Viterbo, P., and Woollen, J.: The ERA-40 re-analysis, Q. J. Roy. Meteor. Soc., 131, 2961–3012, doi:10.1256/qj.04.176, 2005. 1234

van Dop, H., Addis, R., Fraser, G., Girardi, F., Graziani, G., Inoue, Y., Kelly, N., Klug, W., Kulmala, A., Nodop, K., and Pretel, J.: ETEX: a European Tracer Experiment; observations, dispersion modelling and emergency response, Atmos. Environ., 32, 4089–4094, 1998. 1226

GMDD
6, 1223–1257, 2013

Wernli, H. and Davies, H. C.: A Lagrangian-based analysis of extratropical cyclones. I: The method and some applications, Q. J. Roy. Meteor. Soc., 123, 467–489, 1997. 1225, 1227, 1229

Whitaker, J. S., Uccellini, L. W., and Brill, K. F.: A model-based diagnostic study on the rapid development phase of the Presidents' Day Cyclone, Mon. Weather Rev., 116, 2337–2365, 1988. 1225

Würsch, M.: Lagrangian based analysis of airflow during föhn in the Alps, Master thesis, ETH Zurich, 2009. 1239

GMDD

6, 1223–1257, 2013

Table 1. Relative runtime increase with respect to the named reference simulation for COSMO simulations with the online trajectory module for 24615 trajectories and 10 trace variables. The simulations were run using 16 processors (COSMO14 and COSMO7) or 128 processors (COSMO2.2).

	Δx = 14 km	Δx = 7 km	Δx = 2.2 km
without trajectory module (reference: COSMO14 without trajectory module)	0.00	3.16	13.2
with trajectory module (reference: COSMO14 without trajectory module)	0.264	3.45	13.6
with trajectory module (reference: simulation without trajectory module)	0.264	0.0681	0.0366

GMDD
6, 1223–1257, 2013

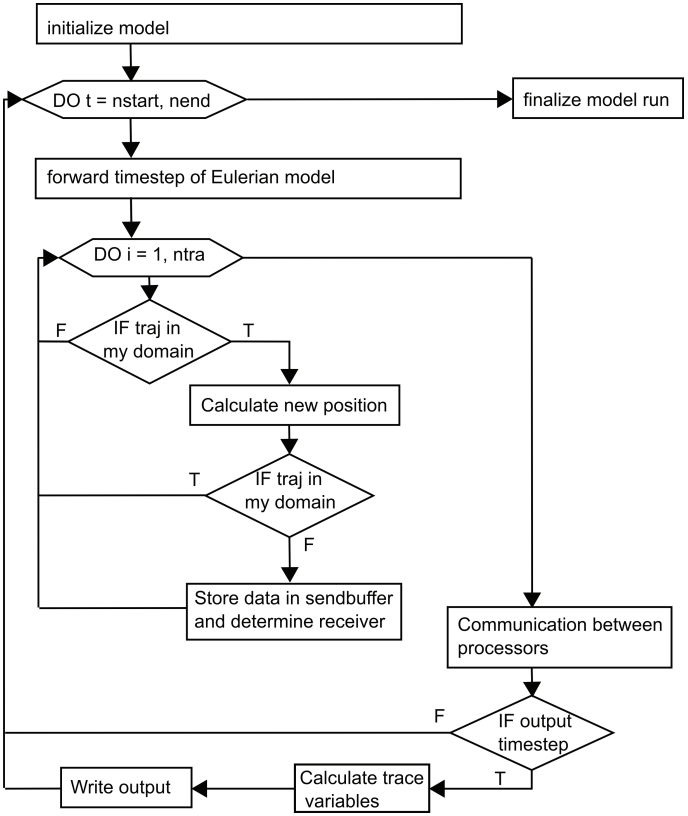

Fig. 1. Flowchart of the online trajectory module for the COSMO model.

GMDD
6, 1223–1257, 2013

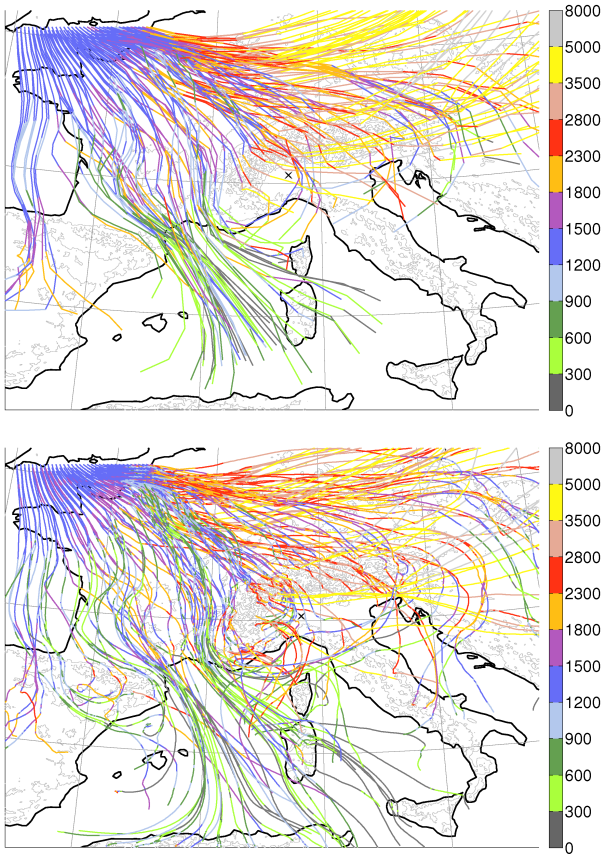

Fig. 2. Offline trajectories based on three-hourly output (top) and online trajectories (bottom) calculated for a COSMO2.2 simulation. Only trajectories starting south of 8.5° N (rotated coordinates) and between 1400 m and 1500 m altitude are shown. The colors denote the height of the trajectories above sea-level (in meters). The trajectories that pass close to the black star are the Föhn trajectories in both panels.

GMDD
6, 1223–1257, 2013

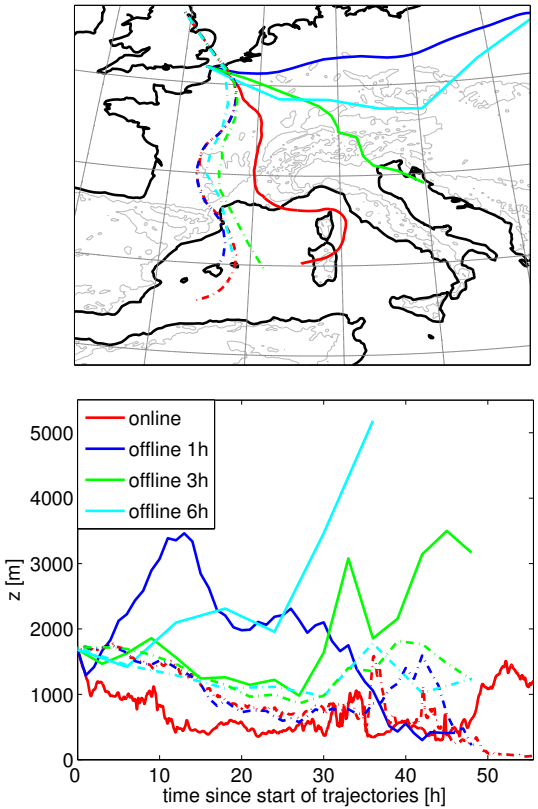

Fig. 3. Example comparisons of online (red) and offline trajectories based on one- (blue), three- (green) and six-hourly (cyan) COSMO model output starting at the same position calculated for the simulation with $\Delta x = 2.2$ km. The two examples (solid and dashed-dotted lines) illustrate extreme cases of similar and divergent trajectories calculated from wind data available at different temporal frequencies.

GMDD
6, 1223–1257, 2013

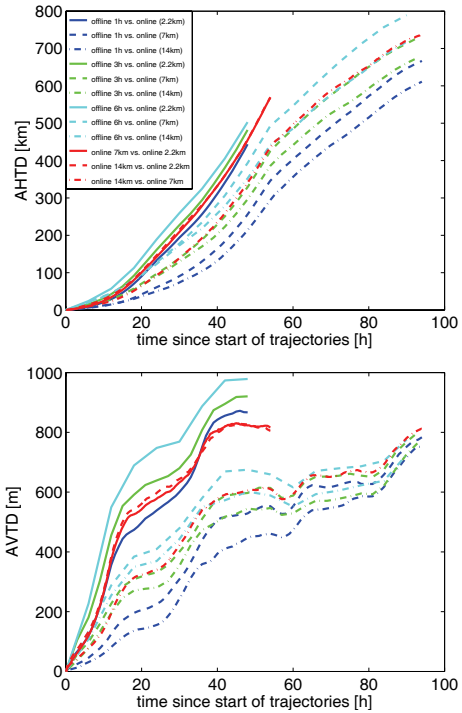

Fig. 4. Average horizontal (top) and vertical (bottom) transport deviation for different trajectory data set pairs (AHTD and AVTD, respectively). Online trajectories are used as reference trajectories and offline trajectories with a data input intervall of 1 h (blue), 3 h (green) and 6 h (cyan) as test trajectories. This comparison is done for horizontal resolutions of the COSMO simulation of $\Delta x = 14$ km (dashed-dotted lines), $\Delta x = 7$ km (dashed lines) and $\Delta x = 2.2$ km (solid lines). In addition online trajectories computed for different spatial resolutions are compared, i.e. $\Delta x = 2.2$ km vs. $\Delta x = 7$ km (solid red line), $\Delta x = 2.2$ km vs. $\Delta x = 14$ km (dashed red lines) and $\Delta x = 7$ km vs. $\Delta x = 14$ km (dashed-dotted red lines). The calculated AHTD(t) and AVTD(t) takes into account all trajectories that are inside the model domain at time t in the test and reference data set.

GMDD
6, 1223–1257, 2013

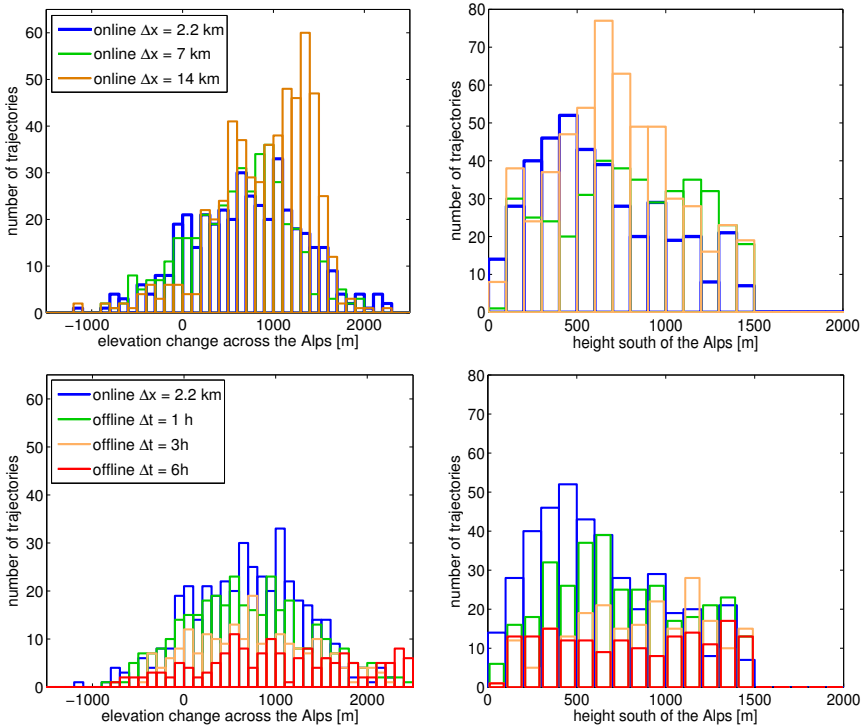

Fig. 5. Histogram of the height difference of the trajectories between the southern and the northern side of the Alps (left panels) and of the height of the trajectories on the southern side of the Alps (right panels). In the top panels the distribution of heights is compared for online trajectories based on simulations with different horizontal resolutions and in the bottom panels online and offline trajectories based on COSMO2.2 are compared.

GMDD
6, 1223–1257, 2013

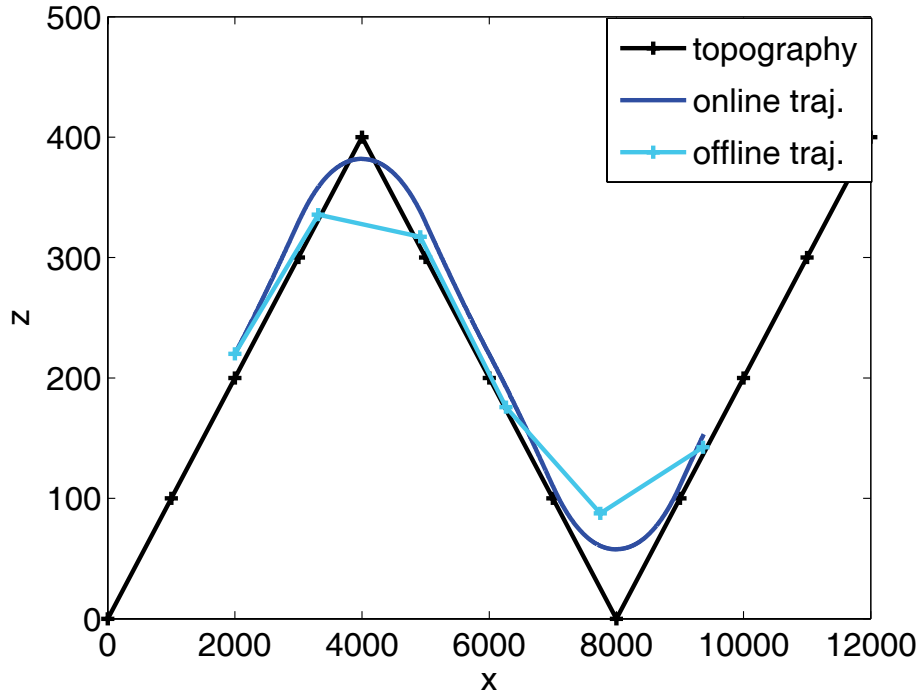

Fig. 6. Illustration of the terrain intersection problem. For the calculation a zic-zac shaped topography is assumed (black line); the wind is assumed to be terrain following and linearly increasing with elevation above ground. The blue line shows the calculated online trajectory and the cyan line an offline trajectory.

GMDD
6, 1223–1257, 2013

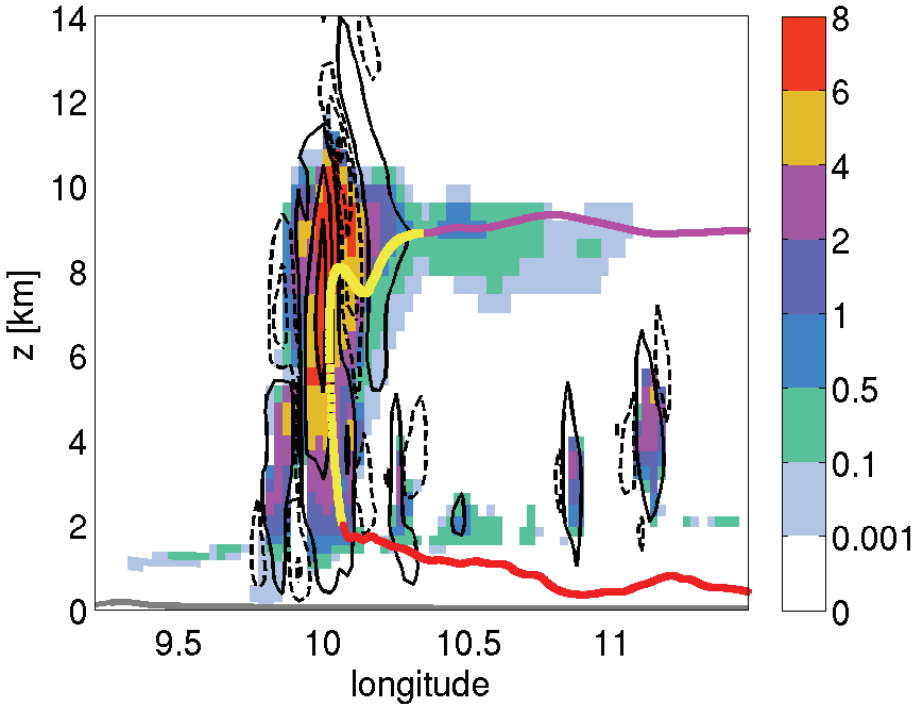

Fig. 7. Online trajectory ascending in a deep convective cloud in the COSMO2.2 simulation over the southern Po Valley in the evening of the 26 July 1987. The colors denote the position of the trajectory relative to the W–E oriented vertical section at 45° N (yellow: in the plane, red: further north, magenta: further south). The color shading shows the total hydrometeor content in $g\,kg^{-1}$ and the contours indicate vertical velocity (solid: upward motion, dashed: downward motion) at 20:00 UTC 26 July 1987, which is the model output time step closest to the ascent of the parcel.

GMDD
6, 1223–1257, 2013